Putting a New Spin of G4 Structure and Binding by Analytical Ultracentrifugation

William L. Dean, Robert D. Gray, Lynn DeLeeuw, Robert C. Monsen and Jonathan B. Chaires*

James Graham Brown Cancer Center
University of Louisville
505 S. Hancock St.
Louisville, KY 50206

Email: j.chaires@louisville.edu

Abstract

Analytical ultracentrifugation is a powerful biophysical tool that provides information about G-quadruplex structure, stability and binding reactivity. This chapter provides a simplified explanation of the method, along with examples of how it can be used to characterize G4 formation and to monitor small-molecule binding.

Key words: Analytical ultracentrifugation, G-quadruplex, Molecular weight, Ligand binding, Stoichiometry, Sample homogeneity

1. Introduction

Analytical ultracentrifugation (AUC) is underappreciated by the G-quadruplex (G4) community. AUC is a venerable biophysical technique that has a (nearly) one-hundred year history. Theodor Svedberg invented the analytical ultracentrifuge in 1925, and won the Noble Prize in Chemistry the next year for his research on colloids and protein using his invention. AUC has since been widely used as a fundamental technique for the determination of macromolecular structure, reaction stoichiometry and ligand affinity [1-4]. AUC is based on first-principle physical theory, and can be used to determine absolute molecular weights of molecules, along with their hydrodynamic shapes. Our laboratory has found AUC useful for a variety of G4 structural studies [5-13]. The intent of this chapter is to provide a simplified overview of AUC and then to show its utility for characterizing G4 structure and binding.

Figure 1 shows a schematic of the most basic AUC experiment, sedimentation velocity (SV). A sample is placed in one sector of centerpiece within a sealed cell assembly with quartz windows (Figure 1A). A reference solution is placed in the second sector. The cell assembly is then placed in a rotor and spun in an ultracentrifuge to produce a high centrifugal field. The centrifugal field is sufficient to cause the sedimentation of molecules within the sample cell in the direction of the field, toward the bottom of sector. The AUC instrument uses an optical system, typically absorbance, to scan the sample cell to monitor the concentration of molecules at each radial position in the cell, and to record their movement as a function of time at constant centrifugal force. As molecules move within the sample cell, a boundary is formed that changes with time. Figure 1B shows a schematic of an SV experiment, with intermittent scans showing the migration of a boundary toward the bottom of the sample cell. As the boundary migrates to the bottom it also broadens because of diffusion of the sedimenting molecule. Such primary data contain sufficient information to extract the structural properties of the sedimenting molecules.

As any number of basic textbooks derive and show, the sedimentation coefficient (s) is defined as the velocity (v) of the moving boundary (determined at the midpoint) divided by the centrifugal field strength ($\omega^2 r$):

$$s = \frac{v}{\omega^2 r} = \frac{M(1 - \bar{v}\rho)}{Nf}$$

The sedimentation coefficient is then equal to product of the molecular weight of the molecule (M) and the buoyancy term ($1 - \bar{v}\rho$) divided by the product of Avagadro's number (N) and the frictional coefficient (f). In the buoyancy term, $\bar{v}$ is the partial specific volume and ρ is the density of the solvent. The sedimentation coefficient is thus determined by the mass of the molecule and its shape. A useful extension of this basic equation is the *Svedberg equation*:

$$\frac{s}{D} = \frac{M(1 - \bar{v}\rho)}{RT}$$

where D is the diffusion coefficient of the molecule, R the gas constant and T the absolute temperature. The molecular weight thus can be obtained from experimentally measured sedimentation and diffusion coefficients.

Mass spectrometry shares with AUC the ability to determine absolute molecular weights of G4 molecules. Both methods can be used to evaluate sample homogeneity or to determine strand stoichiometry and ligand binding. AUC, however, offers some unique advantages. First, AUC measurements are done in solutions of defined and invariant composition, and sedimentation is sensitive to not only the mass of molecules but also their hydrodynamic shape. Second, as molecules are separated in mass spectrometry the equilibrium of the initial sample solution is necessarily perturbed, perhaps leading to some strand dissociation in multi-stranded G4 structures or small-molecule ligand dissociation. In contrast, in AUC measurements the moving G4 boundary remains in equilibrium as it moves through the cell, minimizing perturbation of multi-stranded structures or of bound ligand.

2. Materials

Oligonucleotides were from IDT, Coralville, IA or Eurofins Genomics, Louisville, KY. Stock solutions were prepared by dissolving the lyophilized, desalted oligos in MQ-$H_2$0 to a final concentration of ~1 mM. Working samples were prepared by diluting the stock DNA to ~3-5 µM in the appropriate buffer. In sample preparation, the annealing protocol used can play an important role in quadruplex formation [14]. All samples except those at pH 11.5 were annealed by heating for 5-10 min in a 1-liter boiling water bath followed by slow (12–24 h) cooling to room temperature.

3. Methods

3.1 Analytical ultracentrifugation

Operation of the analytical ultracentrifuge does not lend itself to simple step-by-step protocols. Mastery of the method requires some practice, and is best learned by the study of an excellent tutorial available at: http://www.analyticalultracentrifugation.com/sedphat/experimental_protocols.htm We have presented detailed protocols for the analysis of AUC data obtained for G4 structures in a previous volume of this series [13] and elsewhere [6].

3.2 Illustrative Results

Figure 2 shows an example of experimental data obtained by sedimentation velocity of the "hybrid" G4 structure formed by the human telomere repeat sequence Tel22, 5'AGGG(TTAGGG)$_3$. With modern AUC instrumentation, digital data are collected and

advanced software packages like SEDFIT or UltraScan can be used to fit the data in sophisticated ways to obtain s and D coefficients simultaneously, thereby providing both molecular weight estimates and shape information from a single sedimentation experiment. Figure 2B shows the results of such an analysis, presented as a c(s) plot in which the best-fit distribution of sedimentation coefficients derived from the data is shown. The results show that this G4 sample is homogeneous with a sedimentation coefficient of 1.9S.

3.3 Application of SV to demonstrate G4 structural formation

Figure 3 shows how SV can be used to demonstrate folding of an oligonucleotide into a compact structure. The telomeric sequence d[TTGGG(TTAGGG)$_3$A] has been shown to fold into a compact 3 tetrad hybrid structure termed 2GKU in the presence of K$^+$ [15]. We used AUC to show the different sedimentation behaviors of the unfolded sequence in LiCl, the unfolded sequence at pH 11.5, the folded 2GKU sequence in K$^+$, an unstructured sequence of similar molecular weight, dT$_{24}$, and finally the duplex formed with its complementary sequence. The differences in sedimentation behavior reflect differences in structure, not molecular weight, except for the case of the duplex. As indicated by the equation for the sedimentation coefficient above, an increase in the frictional coefficient due to unfolding will decrease the observed sedimentation coefficient as shown for 2GKU in Li$^+$, at pH 11.5 and for the dT$_{24}$ sequence. The fact that 2GKU in Li$^+$ has a larger sedimentation coefficient than the sequence at pH 11.5 or dT$_{24}$ suggests that some folding has been retained in Li$^+$. The sedimentation coefficient of the duplex is increased due to the near doubling of molecular weight.

The structures of 2GKU under the buffer conditions used for AUC were analyzed by circular dichroism as shown in Figure 3A. The conclusions with respect to oligonucleotide folding are consistent with the CD spectra presented in Figure 3A. For example, 2GKU in 185 mM KCl is fully folded into a hybrid-1 structure, while 2GKU in 180 mM LiCl gives a CD spectrum that indicates partial folding, probably a mixture of folded hybrid and unfolded forms. This is consistent with the known inability of Li$^+$ to promote full G4 folding at these concentrations, but is inconsistent with the prevalent notion that Li$^+$ is *completely* unable to promote G4 folding. As expected, 2GKU in 185 mM KCl, pH 11.5, is unfolded as indicated by CD. The GC-rich 2GKU duplex at neutral pH gives a CD spectrum characteristic of A-type DNA [16] while the CD spectrum of dT$_{24}$ reflects the inherent asymmetry of the nucleobase chromophore itself in an non-helical (random) backbone conformation.

3.4 Detecting and characterizing G4 heterogeneity

A distinct and powerful advantage of SV is its ability to reveal and characterize heterogeneity. Figure 4 shows a case where a truncated form of the human telomere repeat sequence (5'(TTAGGG)$_3$) was studied. It was anticipated that this sequence would fold into a triple-helical structure that might represent an intermediate along the multistate G4 folding pathway. SV shows, however, that this is not the case. There are two structures present at sedimentation coefficients of approximately 1.25 and 2.0 S

4

and calculated molecular weights indicating a mixture of nearly equal amounts monomer and dimer. The CD spectrum (Figure 4 insert) is consistent with a mixture of conformations rather than that of a single structure. This result is expected based on the NMR studies of truncated Tel22 sequences [17].

3.5 Application of SV to show ligand and protein binding to G4 structures

3.5.1 General comments and considerations

Since the seminal paper by Steinberg and Schachman that described the use of the AUC absorbance optical system for studies of small-molecule binding to proteins [18], there have been myriad examples where AUC has been used to determine binding stoichiometry and dissociation constants for protein binding interactions. However, the use of AUC to study interactions between small molecules and DNA is highly underutilized, even though it was first used in 1954 (!) to show that methyl green binds to calf thymus DNA [19]. There are a few published examples utilizing AUC to study small molecule interactions with DNA [20,21,14] , and even fewer assessing interaction of small molecules with G quadruplex-containing sequences [14,22] .

The use of AUC to study small molecule-macromolecule interactions is based on first principles of thermodynamics. The determination of free and bound ligand using SV is actually quite straightforward if the ligand can be detected by absorbance, fluorescence or interference optical systems. Macromolecule and ligand are mixed and allowed to come to equilibrium. The resulting solution is then centrifuged in the AUC. After centrifugation for long enough to separate the faster sedimenting macromolecule from the much slower sedimenting ligand, the free concentration of the ligand can be determined directly from the portion of solution in the centrifuge cell that is free of macromolecule. Knowing the total amount of starting ligand, the amount bound ligand is calculated by difference. An idealized example is shown in Figure 5. This measurement provides the fractional saturation of the ligand at the total ligand concentration used in the experiment and a single point in a binding isotherm that can be used to determine the dissociation constant for the ligand. In addition one can obtain the stoichiometry of binding if the macromolecule is saturated, and an indication of any conformational change in the macromolecule that has occurred upon ligand binding based on changes in the sedimentation coefficient and frictional ratio. This methodology is analogous to equilibrium dialysis and to the classic Hummel and Dryer gel filtration chromatography binding method [23]. A major advantage of AUC over these other methods is that it allows for the analysis of systems free in solution without the possible complications of interactions with a matrix that can occur in gel filtration or the dialysis membrane. Furthermore, one also obtains structural information about the macromolecule in the presence of bound ligand.

If there is overlap between the absorption spectra of the ligand and macromolecule, then a multi-wavelength approach can be used to determine the amounts of ligand and macromolecule in the region of the cell containing both ligand and macromolecule [24-27]. For a two component system such as a single macromolecule and ligand, only two

5

wavelengths are required to determine the contribution of macromolecule and ligand to each position in the centrifuge cell. New methodology has been developed for the most recent iteration of the analytical ultracentrifuge (Beckman Coulter Optima AUC) in which a multi-wavelength scan is acquired at each position in the cell during centrifugation [28]. A general methodology is outlined below.

3.5.2 Steps to determine binding using absorbance optics in the Proteome Lab XL-A

1. The concentration of ligand should be sufficient to give an absorbance of 0.2-1.2.
2. If there is overlap between the absorbance of the ligand and the macromolecule, the experiment must be carried out at two wavelengths, preferably at the absorption maxima of the ligand and the macromolecule. The total absorbance of the two components at each wavelength should be in the range of 0.2-1.2.
3. 430 µL of sample is placed in the sample sector and 450 µL of buffer in the reference sector of a standard 2 sector cell used for sedimentation velocity.
4. A speed of 40,000 rpm is appropriate for most applications with G quadruplex-containing DNA oligonucleotides.
5. Buffers should contain at least 0.1 M salt to minimize non-ideal behavior.
6. To obtain $s_{20,w}$ values and molecular weights, the density and viscosity of the buffer must be known. For simple buffers such as PBS, these parameters can be calculated using the program Sedinterp (free software: http://jphilo.mailway.com/download.htm).
7. Temperature can be maintained between 4 and 40° C in the AUC, but since DNA is quite stable, the standard temperature of 20° C is preferable.
8. Three cells are required for each binding experiment, one containing ligand only at the same concentration as used in the binding experiment, one cell with macromolecule alone at the same concentration used in the mixture, and 1 cell with a mixture of the two components.
9. After centrifugation sufficient for 100 scans (usually 4-8 hours), the data are analyzed by SEDFIT software (www.analyticalultracentrifugation.com) using the continuous c(s) distribution model. The analysis provides the starting concentration of each c(s) vs. s peak so that the concentration of the molecule in the peak can be directly calculated from the extinction coefficient at that wavelength.
10. The starting concentration absorbance for the small molecule is used to determine the free ligand concentration using the extinction coefficient and knowing the total small molecule concentration allows for calculation of bound ligand by difference.

3.5.3 Analysis

Let L_T = total added ligand concentration, L_f = concentration of free ligand, L_b = concentration of bound ligand and M = total added macromolecule concentration in the cell containing the mixture of components. Also let $A°_L$ = the absorbance of the ligand in

the absence of macromolecule and ε_{Lf} = the extinction coefficient of the free ligand so that $L_T = A°_L/\varepsilon_{Lf}\cdot l$ where l is the pathlength of the centrifuge cell (1.2 cm).

A_{Lf} = the absorbance of the free ligand after sedimentation of the mixture so that $L_b = L_T - L_f = A°_L/\varepsilon_{Lf}\cdot l - A_{Lf}/\varepsilon_{Lf}\cdot l$.

Then θ, fractional saturation = $L_b/L_f + L_b$ and $\bar{v}$(moles bound ligand/mole of macromolecule) = L_b/M.

3.5.4 Illustrative Results

.An example of a binding experiment in which interaction between a chemotherapeutic drug, Sunitinib and Tel48 (TTAGGG)$_8$ is shown in Figure 6. At 418 nm only the drug absorbs, so the analysis is not complicated by the presence of Tel48 and looks similar to the idealized example in Figure 5 A. The concentration of free Sunitinib can be calculated directly from the absorbance at 418 nm after sedfit analysis in the continuous c(s) distribution model in which the area under the c(s) vs s peak is equal to the absorbance of that species (Figure 6B). Note that the absorbance for free Sunitinib from a single scan in Figure 6A is equal to the absorbance in the integrated peak in Figure 6B. In this experiment the starting concentration of Sunitinib was 30 µM and Tel48 was 3 µM, so at this 10-fold excess of drug, the apparent stoichiometry is 6.3 moles of drug/mole Tel48.

Table 1 summarizes the results for a number of small molecules found to interact with different G4 structures, including an antiparallel hybrid form (Tel 22), a structure containing contiguous antiparallel G4 structures (Tel48) and a parallel, "propeller" G4 structure (1XAV). The reliable determination of the binding stoichiometries show in Table 1 provides a firm foundation for the analysis of binding isotherms obtained by independent spectrophotometric titrations or by isothermal calorimetry.

4. Final Comments

Our laboratory now regards AUC as an essential criterion for the demonstration of G4 formation in nucleic acid sequences of interest. AUC shows definitively whether or not a given sequence has folded into a compact structure and then provides the molecular weight of the structure to unambiguously determine its molecularity. AUC provides a clear characterization of the homogeneity of the folded structure, and clearly identifies the presence and exact amounts any unfolded species or unwanted aggregates. AUC clearly indicates if additional sample purification is needed. Once AUC has established that a sequence has folded into a homogeneous structure, additional methods like circular dichroism can be used with confidence to characterize the topological features of the folded G4 structure [29]. Our confidence in AUC as a biophysical tool based on fundamental physical principles is such that we have adopted the motto "*AUC non mentior*" – AUC does not lie.

Acknowledgement

Table I. Summary of Small Molecule Binding AUC measurements in K⁺ buffers

Compound	DNA	Stoichiometry*	Wavelength
Sunitinib	Tel22	3	415
	Tel48	12	415
	1XAV	5	415
Doxorubicin	Tel48	12	470
Berberine	Tel22	1	345
	Tel48	2	345
Ceritinib	Tel22	5	310
Osimertinib	Tel22	3	310
	Tel48	4	320
Ponatinib	Tel22	3	310
	Tel48	7	320
Thiazole orange	Tel22	3	478
	1XAV	3	478
NMM	Tel22	0	380
	1XAV	1	380
Quindoline	Tel22	4	340
	1XAV	4	340
Crizotinib	Tel22	2	315
	Tel48	6	315
Bosutinib	Tel22	0	340
	Tel48	1	340
Afatinib	Tel22	1	346
	Tel48	4	346
Capecitabine	Tel22	1	300
	Tel48	2	300
Palbociclib	Tel22	1	350
	Tel48	4	350

*Rounded to nearest whole number. Ratio of small molecule:DNA for all experiments was a minimum of 10.

References

1. Schachman HK (1959) Ultracentrifugation in Biochemistry. Academic Press, New York

2. Uchicyama S, Arisaka F, Stafford WF, Laue T (2016) Analytical Ultracentrifugation Instrumentation, Sofware and Allications. Spinger, Japan

3. Schuck P, Zhao H, Brautigam CA, Ghirlando R (2016) Basic Principles of Analytical Ultracentrifugation. CRC Press, Boca Raton, FL

4. Schuck P, Zhao H (2018) Sedimentation Velocity Analytical Ultracentrifugation: Interacting Systems. CRC Press, Boca Raton, FL

5. Li J, Correia JJ, Wang L, Trent JO, Chaires JB (2005) Not so crystal clear: the structure of the human telomere G-quadruplex in solution differs from that present in a crystal. Nucleic Acids Res 33 (14):4649-4659. doi:10.1093/nar/gki782

6. Chaires JB, Dean WL, Le HT, Trent JO (2015) Hydrodynamic Models of G-Quadruplex Structures. In: Cole JL (ed) Analytical Ultracentrifugation, vol 562. Methods in Enzymology. pp 287-304. doi:10.1016/bs.mie.2015.04.011

7. Chaires JB, Trent JO, Gray RD, Dean WL, Buscaglia R, Thomas SD, Miller DM (2014) An improved model for the hTERT promoter quadruplex. PLoS One 9 (12):e115580. doi:10.1371/journal.pone.0115580

8. Le HT, Buscaglia R, Dean WL, Chaires JB, Trent JO (2013) Calculation of Hydrodynamic Properties for G-Quadruplex Nucleic Acid Structures from in silico Bead Models. In: Chaires JB, Graves D (eds) Quadruplex Nucleic Acids, vol 330. Topics in Current Chemistry. pp 179-210. doi:10.1007/128_2012_351

9. Mekmaysy CS, Petraccone L, Garbett NC, Ragazzon PA, Gray R, Trent JO, Chaires JB (2008) Effect of O6-methylguanine on the stability of G-quadruplex DNA. J Am Chem Soc 130 (21):6710-6711. doi:10.1021/ja801976h

10. Petraccone L, Garbett NC, Chaires JB, Trent JO (2010) An integrated molecular dynamics (MD) and experimental study of higher order human telomeric quadruplexes. Biopolymers 93 (6):533-548. doi:10.1002/bip.21392

11. Petraccone L, Spink C, Trent JO, Garbett NC, Mekmaysy CS, Giancola C, Chaires JB (2011) Structure and stability of higher-order human telomeric quadruplexes. J Am Chem Soc 133 (51):20951-20961. doi:10.1021/ja209192a

12. Petraccone L, Trent JO, Chaires JB (2008) The tail of the telomere. J Am Chem Soc 130 (49):16530-16532. doi:10.1021/ja8075567

13. Garbett NC, Mekmaysy CS, Chaires JB (2010) Sedimentation velocity ultracentrifugation analysis for hydrodynamic characterization of G-quadruplex structures. Methods Mol Biol 608:97-120. doi:10.1007/978-1-59745-363-9_7

14. Le HT, Miller MC, Buscaglia R, Dean WL, Holt PA, Chaires JB, Trent JO (2012) Not all G-quadruplexes are created equally: an investigation of the structural polymorphism of the c-Myc G-quadruplex-forming sequence and its interaction with the porphyrin TMPyP4. Org Biomol Chem 10 (47):9393-9404. doi:10.1039/c2ob26504d

15. Luu KN, Phan AT, Kuryavyi V, Lacroix L, Patel DJ (2006) Structure of the human telomere in K+ solution: an intramolecular (3 + 1) G-quadruplex scaffold. J Am Chem Soc 128 (30):9963-9970. doi:10.1021/ja062791w

16. Kypr J, Kejnovska I, Renciuk D, Vorlickova M (2009) Circular dichroism and conformational polymorphism of DNA. Nucleic Acids Res 37 (6):1713-1725. doi:10.1093/nar/gkp026

17. Zhang N, Phan AT, Patel DJ (2005) (3 + 1) Assembly of three human telomeric repeats into an asymmetric dimeric G-quadruplex. J Am Chem Soc 127 (49):17277-17285. doi:10.1021/ja0543090

18. Steinberg IZ, Schachman HK (1966) (- 1966/12/01). - 5 (- 12):- 3747

19. Kurnick NB (1954) (- 1954/01/01). - 76 (- 2):- 424

20. Chaires JB (1983) Equilibrium studies on the interaction of daunomycin with deoxypolynucleotides. Biochemistry 22 (18):4204-4211

21. Sprigg L, Li A, Choy FY, Ausio J (2010) Interaction of daunomycin with acetylated chromatin. J Med Chem 53 (17):6457-6465. doi:10.1021/jm1007853

22. Gao Y, Guang T, Ye X (2017) Sedimentation velocity analysis of TMPyP4-induced dimer formation of human telomeric G-quadruplex. RSC Advances 7 (87):55098-55105. doi:10.1039/C7RA07758K

23. Hummel JP, Dreyer WJ (1962) Measurement of protein-binding phenomena by gel filtration. Biochimica et Biophysica Acta 63 (3):530-532. doi:https://doi.org/10.1016/0006-3002(62)90124-5

24. Padrick SB, Brautigam CA (2011) Evaluating the stoichiometry of macromolecular complexes using multisignal sedimentation velocity. Methods 54 (1):39-55. doi:10.1016/j.ymeth.2011.01.002

25. Padrick SB, Deka RK, Chuang JL, Wynn RM, Chuang DT, Norgard MV, Rosen MK, Brautigam CA (2010) Determination of protein complex stoichiometry through multisignal sedimentation velocity experiments. Anal Biochem 407 (1):89-103. doi:10.1016/j.ab.2010.07.017

26. Zhao H, Brautigam CA, Ghirlando R, Schuck P (2013) Overview of current methods in sedimentation velocity and sedimentation equilibrium analytical ultracentrifugation. Curr Protoc Protein Sci Chapter 20:Unit20 12. doi:10.1002/0471140864.ps2012s71

27. Gorbet GE, Pearson JZ, Demeler AK, Colfen H, Demeler B (2015) Next-Generation AUC: Analysis of Multiwavelength Analytical Ultracentrifugation Data. Methods Enzymol 562:27-47. doi:10.1016/bs.mie.2015.04.013

28. Pearson JZ, Krause F, Haffke D, Demeler B, Schilling K, Colfen H (2015) Next-Generation AUC Adds a Spectral Dimension: Development of Multiwavelength Detectors for the Analytical Ultracentrifuge. Methods Enzymol 562:1-26. doi:10.1016/bs.mie.2015.06.033

29. Del Villar-Guerra R, Trent JO, Chaires JB (2018) G-Quadruplex Secondary Structure Obtained from Circular Dichroism Spectroscopy. Angew Chem Int Ed Engl 57 (24):7171-7175. doi:10.1002/anie.201709184

30. Del Villar-Guerra R, Gray RD, Chaires JB. (2017) Curr Protoc Nucleic Acid Chem. 68:17.8.1-17.8.16. doi: 10.1002/cpnc.23.

Figure Legends

Figure 1. Schematic representation of a sedimentation velocity experiment. The panel on the left represents a double sector centrifuge cell with a sedimenting sample in the upper sector and the reference buffer in the lower sector. The right panel shows four absorbance scans taken at four different times during sedimentation.

Figure 2. Sedimentation velocity experiment showing results from a solution containing 5 µM Tel22 in 0.2 M KCl. Panel A shows the raw data from 23 of the 100 scans taken over a 6 hour time period at 40,000 rpm and 20°C. Panel B shows sedfit analysis using the continuous c(s) distribution model. The results show that this G4 sample is homogeneous with a sedimentation coefficient of 1.9S.

Figure 3. AUC and CD analysis of 2GKU under various buffer conditions known to result in the formation of different structures. Panel A shows CD spectra of 2GKU in KCl (black), 2GKU in LiCl (blue), 2GKU duplex (red), dT_{24} (green) and 2GKU at pH 11.5 (purple). The buffer was 10 mM sodium phosphate with added 185 mM KCl or LiCl, pH 7.0 or 11.5. Blank-corrected CD spectra were recorded in a 1-cm pathlength quartz cuvette at 25 °C with a Jasco J810 spectropolarimeter equipped with Pelteir temperature controller as described [30]. CD spectra were normalized using the equation $\Delta\varepsilon = \theta/32980 \cdot l \cdot c$ where θ is the observed ellipticity in millidegrees, l is the pathlength in cm and c is the molar strand concentration of DNA. Figure 3B shows sedfit analysis of sedimentation velocity results using the continuous c(s) distribution model of the same solutions using the same color scheme as in 3A.

Figure 4. Sedfit analysis of 5'(TTAGGG)$_3$ (7 µM) in 10 mM MOPS, 30 mM KCl, pH 7.0, using the continuous c(s) distribution model. Inset to Figure 4. CD spectrum of Tel22-5'Δ4 (7 µM) in 10 mM MOPS, 30 mM KCl, pH 7.0.

Figure 5. Idealized binding analysis experiment using sedimentation velocity with absorption optics. Panel A shows the results of a single scan at the wavelength where the receptor absorbs and at a time when the receptor has sedimented approximately 60% of the length of the solution column. Panel B shows the results at the same time at a wavelength where the ligand absorbs. Panel C shows analysis of the scan from panel B with concentrations of total, free and bound ligand clearly delineated.

Figure 6. Sedimentation velocity analysis of binding of Sunitinib to Tel48. Sunitinib (30 µM) was mixed with Tel48 (3 µM) for 30 minutes and then analyzed by sedimentation velocity at 418 nm, the absorbance maximum of Sunitinib. Tel48 does not absorb at that wavelength. Panel A shows binding analysis as described in Figure 5C for a single scan where Tel48 has sedimented 60% of the length of the solution column. Panel B shows sedfit analysis of the binding experiment using the continuous c(s) distribution model. The area under the curve at the sedimentation coefficient of Tel48 represents bound Sunitinib and is exactly equal to the absorbance of bound Sunitinib determined in 6A, 0.28 absorbance units.
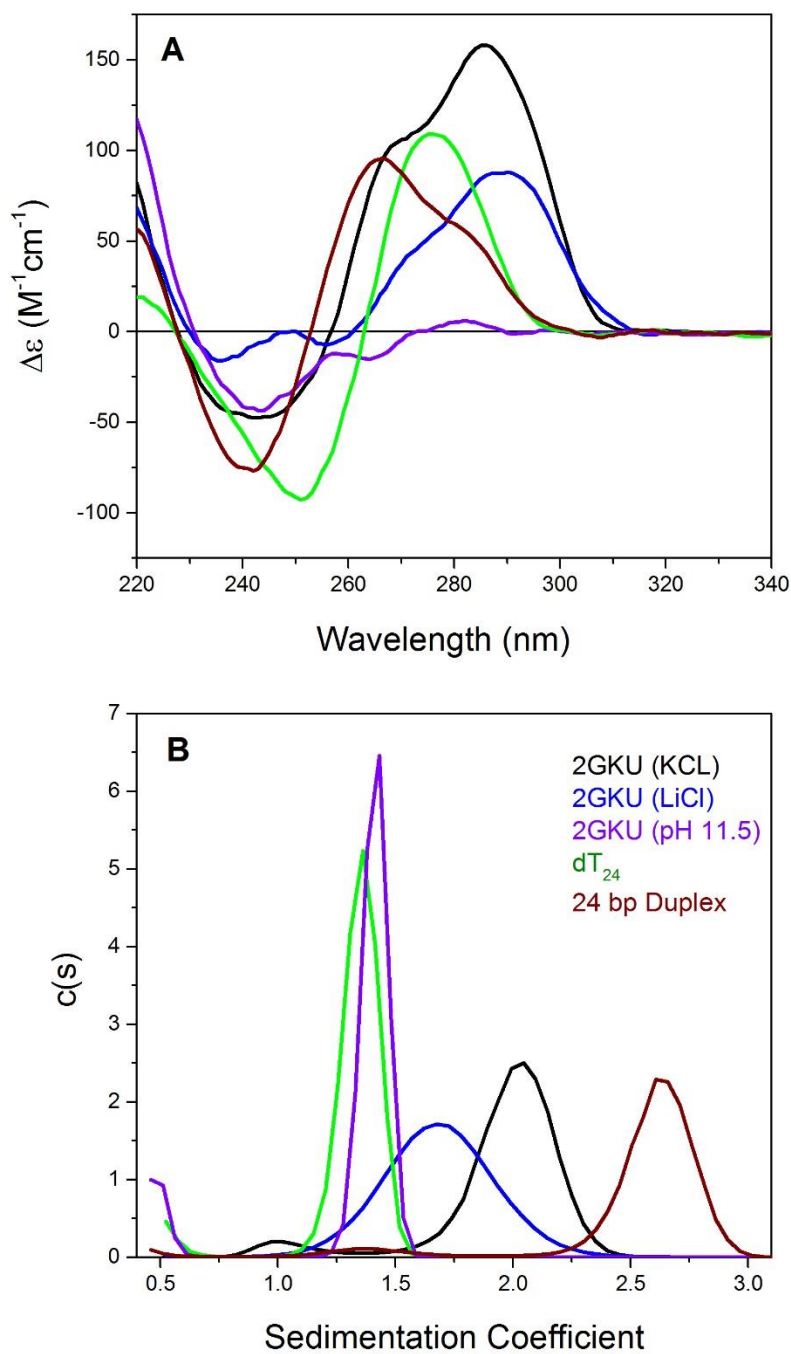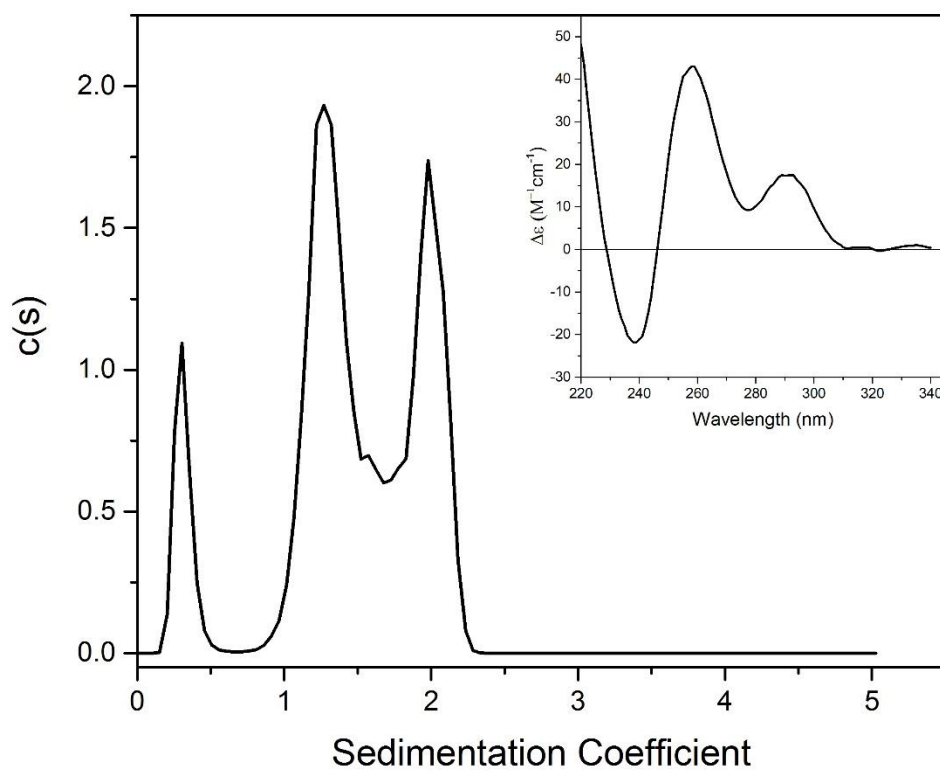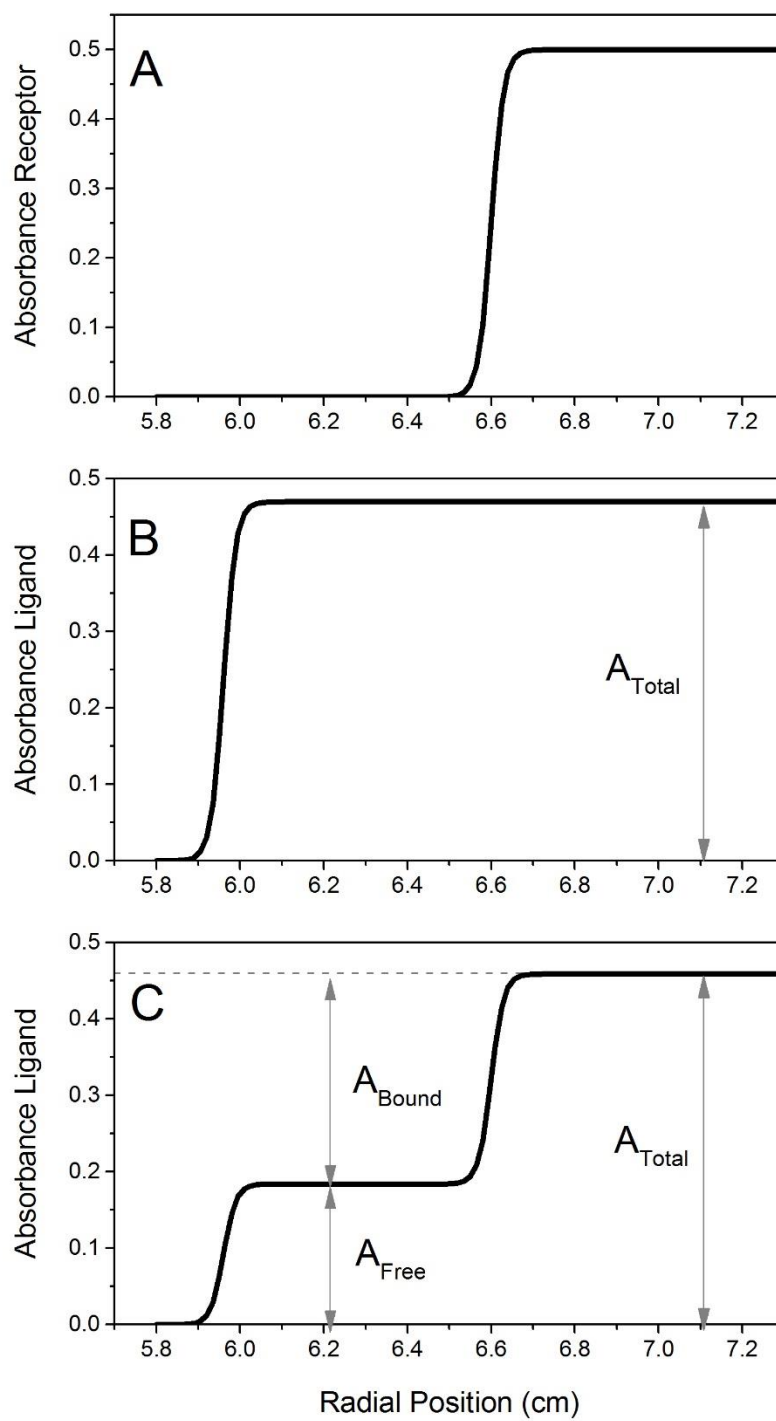
Figure 1
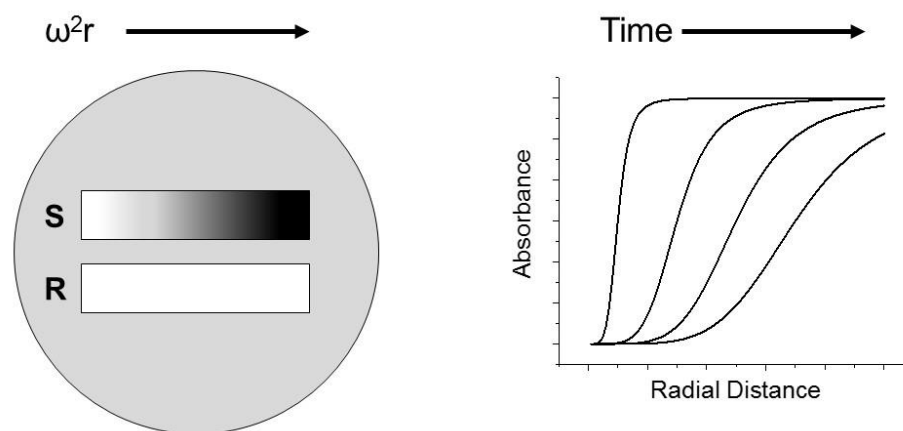
Figure 2
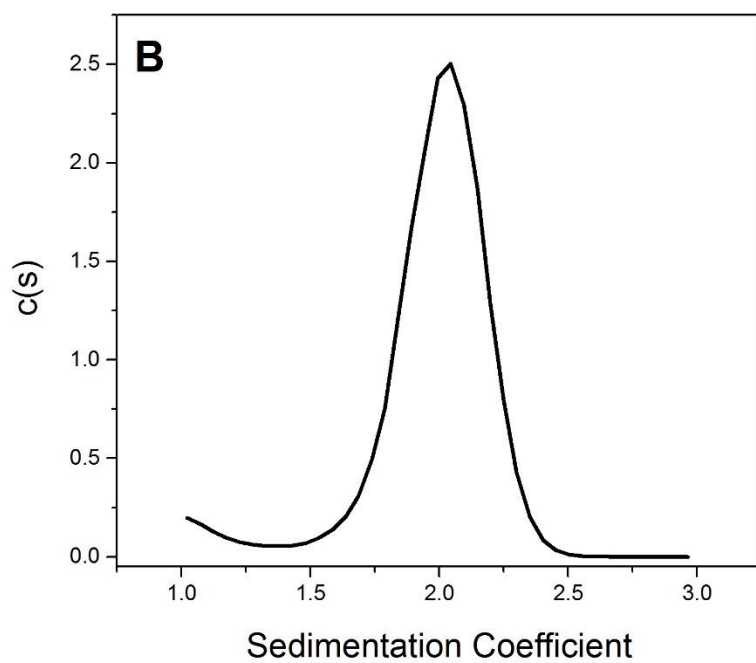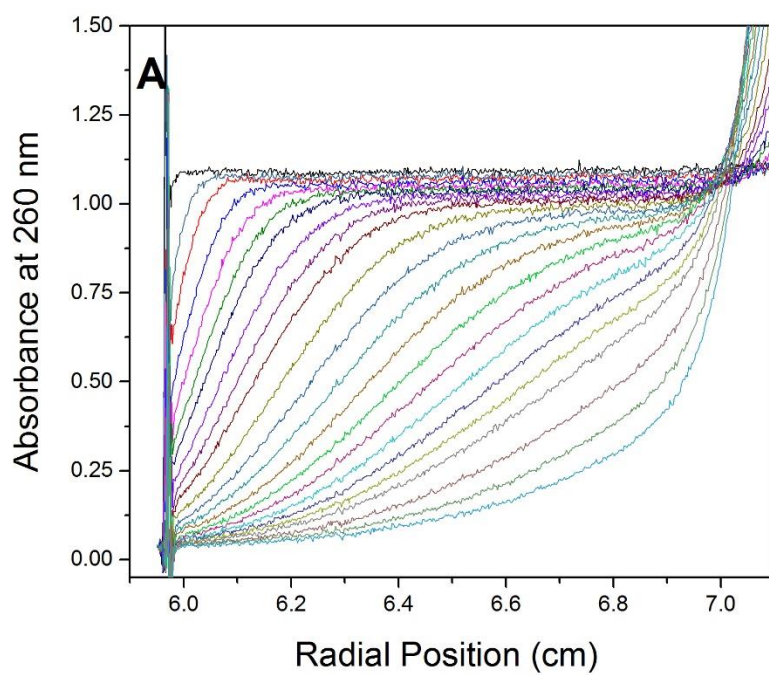
Figure 3

Figure 4

Figure 5

Figure 6